A STUDY OF THE VELOCITY STRUCTURE IN A MARINE BOUNDARY LAYER - INSTRUMENTATION AND OBSERVATIONS

by

JOHN STEVEN TOCHKO

B.E., The Cooper Union School of Engineering
(1972)

SUBMITTED IN PARTIAL FULFILLMENT OF THE
REQUIREMENTS FOR THE DEGREE OF
DOCTOR OF PHILOSOPHY

at the

MASSACHUSETTS INSTITUTE OF TECHNOLOGY

and the

WOODS HOLE OCEANOGRAPHIC INSTITUTION

February 1978

Signature of Author: John S. Tochko

Joint Program in Oceanographic Engineering,
Massachusetts Institute of Technology-Woods Hole
Oceanographic Institution, February 1978

Certified by: Albert J. Williams 3rd

Thesis Supervisor

Accepted by: Earl E. Hays

Chairman, Joint Committee on Oceanographic
Engineering, Massachusetts Institute of Technology-
Woods Hole Oceanographic Institution

A STUDY OF THE VELOCITY STRUCTURE IN A MARINE BOUNDARY LAYER

- INSTRUMENTATION AND MEASUREMENTS

by

John Steven Tochko

Submitted to the Department of Ocean Engineering in partial fulfillment of the requirements for the degree of Doctor of Philosophy.

ABSTRACT

The design and operation of a unique flow measuring instrument for bottom boundary layer studies in the marine environment is documented. The effectiveness of the instrument in acquiring data with which models of near bottom flows in the ocean can be tested is demonstrated by the results of a field experiment in Vineyard Sound.

The instrument uses four sensors which measure the mean and fluctuating parts of the three components of the velocity vector at four heights above the sea bed. The sensors employ the acoustic travel time difference technique, and are designed to minimize sensor-induced flow disturbances. BASS, an acronym for Benthic Acoustic Stress Sensor, has a resolution of .033 cm/sec per least bit, a range of ±62 cm/sec, noise of .07 cm/sec in 10 sec, and an estimated accuracy of ±.5 cm/sec, referred to an in situ zero point. A complete set of velocity measurements is made every .750 seconds, each measurement being the vector component averaged over 15 cm. The data is internally recorded on digital cassette tape. Eight hours of continuous data can be recorded.

BASS was deployed in a tidal flow in Vineyard Sound at a depth of 10 m where a time series of u, v, and w velocities at 26 cm, 46 cm, 96 cm, and 210 cm above the bottom was recorded. The mean velocity was determined by fitting each 6 hour series with a sixth order polynomial and the deviations from the polynomial, the fluctuating velocity components, were correlated to produce Reynolds stress profiles. The stress series shows very few negative stress events while the dominant positive events have an average duration of 5 seconds and exceed 30 dynes/cm^2.

Zero offset was removed from the mean by assuming a log profile at maximum ebb. Deviations from a log profile developed when the current dropped below 40% of maximum, i.e., when the flow could no longer be considered steady. A break in the Reynolds stress profile at 1 m suggested a larger length scale than the 1 cm bottom roughness was present in the flow. A value of u_* was determined by using the quadratic drag law (u_* = 1.56 cm/sec), the log profile method (u_* = 1.60 cm/sec), and the

eddy correlation method (u_* = 1.91 cm/sec). Integral length scales of 5 m cross-stream, and 2.5 m vertically were identified by correlation calculations. Two length scales were present in the downstream direction, 5 m within 1 meter of the wall and 8 m further from the wall.

Thesis Supervisor: Albert J. Williams 3rd
Title: Associate Scientist

ACKNOWLEDGEMENTS

Dr. Albert J. Williams 3rd helped me in many ways during the course of this work. He not only guided my academic progress, but also came to my rescue when I had technical difficulties with the instrumentation or with my automobile. I am grateful to him for the key role he played in getting BASS off the drawing board and into the ocean.

The technicians and engineers of the Ocean Engineering Instrument Section provided sound technical advice in the design and construction phases of this project.

Dr. Brad Butman of the U.S. Coast and Geodetic Survey provided the mounting frame for the instrument.

Tim Fofonoff and Jacob Ladderman helped with the preparations for the field experiment.

Woods Hole divers, Dr. William Grant and Matthew Greer provided valuable field observations and photographs. I thank Dr. Grant for his critical reviews of the early drafts of the text.

Captain Roy Campbell and the crew of the M.V. Whitefoot made the field deployment procedure work faultlessly.

Dr. Robert Spindel generously allowed me the use of his project's computer for the data analysis.

Karen Pires prepared early drafts of the text, and was assisted by Judith De Santi in typing the final manuscript.

I thank my thisis committee, Dr. G.T. Csanady, Dr. W.L. Harris, Sr., Dr. C.D. Hollister and Dr. O.S. Madsen for their advice and critical

review of the thesis. Dr. I.N. McCave also provided valuable criticism.

Finally I thank my friends Matt Greer, Chris Myles, George Rodenbusch, and James R. Sullivan for their encouragement and help during the course of this thesis. The Woods Hole Oceanographic Institution Education Program patiently supported my work. Support from the National Science Foundation is also acknowledged.

TABLE OF CONTENTS

	Page No.
ABSTRACT	1
ACKNOWLEDGEMENTS	2
LIST OF FIGURES AND TABLES	6
PREFACE	9
1. INTRODUCTION	12
1.1 Turbulent Boundary Layer Scales	14
1.2 Background to Methods of Investigation	25
1.2.1 Quadratic Drag Law	25
1.2.2 Logarithmic Profile Method	27
1.2.3 Reynolds Stress and Eddy Correlation	30
1.2.4 Intermittency	43
1.3 Previous Instrumentation	47
1.4 Summary of Objectives	53
2. INSTRUMENTATION	55
2.1.1 Sensor Requirements	55
2.1.2 Choice of the Acoustic Travel Time Sensor	56
2.2 The Acoustic Travel Time Sensor	59
2.2.1 Basic Technique	59
2.2.2 Mechanical Design	62
2.3 BASS Electronics	67
2.3.1 Transmitter Circuitry	68
2.3.2 Receiver Circuitry	70
2.3.3 Timing Circuitry	76

TABLE OF CONTENTS (cont.) Page No.

2.4 Data Processing. 78

2.5 Sources of Error 82

3. THE EXPERIMENT. 98

3.1 Site Motivation and Location 98

3.2 Deployment and Measurements. 100

4. EXPERIMENTAL RESULTS. 103

4.1 The Data Set 103

4.2 The Mean Flow. 105

4.2.1 Mean Velocity Profiles. 105

4.2.2 Quadratic Drag Law. 111

4.2.3 The Profile Method. 112

4.3 Velocity Fluctuations. 119

4.3.1 Root Mean Square Velocities 125

4.3.2 Measured Reynolds Stresses. 130

4.3.3 Correlations and Integral Scales. 152

4.4 Alternative Validation of Reynolds Stress Measurements . 158

5. SUMMARY AND CONCLUSIONS 165

5.1 BASS 165

5.2 The Mean Flow. 166

5.3 Fluctuations and Reynolds Stress 167

APPENDICES. 171

BIBLIOGRAPHY. 181

BIOGRAPHICAL NOTE 187

LIST OF FIGURES AND TABLES

		Page No.
TABLE 1.1	Boundary Layer Scales.	22
FIGURE 1.1	Schematic Diagram of a Marine Boundary Layer.	23
FIGURE 1.2	Mean Velocity Profiles (after Mosby, 1946).	29
FIGURE 1.3	Definition Sketch of Coordinate System.	32
FIGURE 1.4	Mean Autocorrelation Curves for u and w (after Bowden and Fairbairn (1956)).	37
FIGURE 1.5	Square Root of Bottom Stress Versus Mean Flow Velocity in an Estuary (after Seitz (1971)).	40
FIGURE 1.6	Hysteresis of Reynolds Stress as a Function of Current Speed (after Gordon (1975)).	41
FIGURE 1.7	Sketch of an Ejection and Sweep Event.	45
TABLE 1.2	Summary of Marine Boundary Layer Studies.	49
FIGURE 2.1	Sketch Showing Basic Principle of the Acoustic Travel Time Technique.	61
FIGURE 2.2	Acoustic Travel Time Sensor With Four Sensing Paths.	64
FIGURE 2.3	The Benthic Acoustic Stress Sensor.	66
FIGURE 2.4	Transmitted and Received Waveforms Showing Schmidt Trigger Input and Output.	71
FIGURE 2.5	Receiver Timing Diagram.	73
FIGURE 2.6	Block Diagram of Receiver Circuitry.	74
FIGURE 2.7	Schematic Diagram of BASS Data Path.	81
FIGURE 3.1	Bathymetry of Vineyard Sound Near the BASS Deployment Site.	99
FIGURE 3.2	Density Profiles Computed From SCIMP CTD Data.	102
FIGURE 4.1	Typical Segment of Time Series Showing the u,v, and w velocities at 26 cm Above the Bottom.	104

		Page No.
FIGURE 4.2	Time Series of Horizontal Velocity 96 cm Above the Bottom.	106
FIGURE 4.3a	Profiles of Mean Horizontal Velocity - U Component	108
FIGURE 4.3b	Profiles of Mean Horizontal Velocity - V Component	109
TABLE 4.1	Values of u_* Obtained From the Quadratic Drag Law.	112
FIGURE 4.4	Plot of Log z Versus U	113
TABLE 4.2	Table of Mean U Values and Results from the Log Profile Method	114
TABLE 4.3	Values of u_* at Four Levels Above the Bottom	117
FIGURE 4.5	Plot of u_* Versus Depth Averaged Horizontal Velocity in Vineyard Sound.	118
FIGURE 4.6	Typical Segment of the u,v,w Fluctuating Time Series at 26 cm Above the Bottom.	120
FIGURE 4.7	Time Series of Streamwise (u) Velocity Fluctuations at Four Elevations Above the Bottom	122
FIGURE 4.8	Time Series of Cross-stream (v) Velocity Fluctuations at Four Elevations Above the Bottom.	123
FIGURE 4.9	Time Series of Vertical (w) Velocity Fluctuations at Four Elevations Above the Bottom.	124
FIGURE 4.10	Plots of u_{rms}, v_{rms}, w_{rms} Versus Time.	126
FIGURE 4.11	Plots of Intensity of Turbulent Kinetic Energy Versus Time.	129
FIGURE 4.12	Plots of Intensity of Turbulent Kinetic Energy $q^2/2$ Versus Mean Horizontal Velocity U.	131
FIGURE 4.13	Time Series of u,w, and - uw; 26 cm Above the Bottom.	133

		Page No.
FIGURE 4.14	Time Series of Reynolds Stress at Four Points Above the Bottom.....	135
FIGURE 4.15	Profiles of $-\rho uw$ Reynolds Stress.....	137
FIGURE 4.16	Profiles of $-\ _{vw}$ Reynolds Stress.....	138
FIGURE 4.17	BASS on a 13% Grade.....	145
FIGURE 4.18	BASS in the Wake of a Topographic Feature.....	148
TABLE 4.4	Values of u_* from Turbulent Fluctuation Measurements.....	150
FIGURE 4.19	Reynolds Stress Versus Mean Horizontal Velocity....	151
FIGURE 4.20	Correlation Curves at 210 cm and 26 cm Above the Bottom.....	153
TABLE 4.5	Correlation Coefficients for Three Lag Times.....	154
TABLE 4.6	Integral Scales as a Function of Height Above the Bottom.....	155
FIGURE 4.21	Plots of Integral Scale Lengths Versus Height Above the Bottom.....	156
FIGURE 4.22	Tow Tank Set up.....	161

PREFACE

This thesis documents the development of instrumentation to measure benthic boundary layer flow and its test in a tidal channel in Vineyard Sound. An understanding of the characteristics of bottom boundary layer flows is necessary in order to determine the attributes this instrument must possess to perform its designated task. For this reason, and because this thesis may be read by scientists interested in near bottom flow measurements who are not fluid dynamicists, there is a basic discussion of the scaling parameters of turbulent boundary layers.

The results of the field test are presented as a unique data set in which the three components of the velocity vector at four levels above the seabed were sampled simultaneously with the data being obtained from sensors having an averaging volume with a characteristic dimension of 15 cm. The data are presented and interpreted as a demonstration of the potential of the instrument rather than as a contribution to the understanding of turbulent estuarine boundary layers. The contribution of this thesis is neither the data set nor its interpretation, but rather the proven capability of the instrumentation to make superior measurements from which models can be tested and our knowledge of marine boundary layer flows increased.

The quality of the measurements from this instrument approaches that previously obtainable only from flume studies. The instrument was tested in the sea rather than in a flume for the practical reasons

of economics and availability. Large flumes (deeper than two meters) are generally expensive and unavailable while a nearby natural flow was readily accessible. The individual sensors were tested in a small tow tank, but the real test of the system was its deployment in the ocean. The reason for studying a boundary layer in nature rather than applying laboratory results to natural flows lies in the observation that not enough is known yet about the forcing functions and dynamically important features of natural flows to model them entirely on laboratory measurements. The data collected primarily for the validation of the instrument also shows promise in increasing our understanding of shallow tidal flows under the conditions of the field test.

Finally, the selection of material included in this thesis can best be understood in the context of the events which lead to its completion. In January 1975, I gained familiarity with the instrumentation possibilities of an acoustic shearmeter by assisting in its construction and testing while also learning more about turbulent flows and helping to produce research proposals to develop instrumentation for mearuring deep-sea boundary layer flows. Funding developed in 1976 and I began construction of my prototype designs. The complete instrument was ready for testing in August 1977, and was deployed in Vineyard Sound where the flow is reasonably simple. The data set from this deployment was subjected to computer analysis until early December. Along the way, a suite of programs was generated for data editing, plotting, and analysis, which resulted in plots of many measures of this turbulent flow. Besides valididating the measurement technique, the results were applied

to a simple model of a boundary layer flow which was later expanded to include the effects of unsteadiness and multiple length scales. Additional models and analysis schemes have been brought to my attention through my attempts to interpret the data set. These must however remain the target for future work.

CHAPTER 1

INTRODUCTION

The thrust of the research documented in this thesis has been directed toward achieving two goals: the first is to provide ocean scientists with a unique tool capable of making detailed measurements of the velocity structure in a marine boundary layer, and the second goal is to demonstrate the ability of this instrument to obtain significantly better measurements than can be obtained with existing instruments so that our understanding of boundary layer flow processes can be increased. The motivation behind this stems from the need expressed by investigators in many ocean-related disciplines for engineering data associated with the transport processes in near bottom flows. The dynamics of the flow in the immediate vicinity of the sea bed govern the fluxes of heat, momentum, chemical species, and sediment, and also play a dominant role in the formation and alteration of sediment bedforms. A detailed engineering investigation of the flow parameters in a geophysical boundary layer is necessary to gain insight into such varied problems as the interchange of thermal and kinetic energy between the bottom waters and the sediments, the transport of these sediments, the refraction of acoustic signals, and the operating conditions for engineering projects, oceanographic experiments, contained sea-bed waste disposal and deep sea mining. The interaction of the stresses at the boundary with the interior flow is an important phenomena to understand in order to model the dynamics of the global flow of the interior of the ocean.

Most boundary layer research has been performed in wind tunnels, flumes and in the atmosphere. The relatively few field measurements made in the ocean have used sensors which lacked the ability to simultaneously produce time series of the three components of the velocity vector at various distances from the bottom. Deep sea experiments using visual and mechanical measuring techniques have given only coarse estimates of the flow conditions on the bottom.

The first part of this study presents a summary of the important scales and velocity relationships in turbulent boundary layers, describes methods of investigating the parameters in such a flow in the marine environment, and then traces the design and development of a new instrument capable of supplying velocity data crucial to the understanding of marine boundary layer processes. The instrument represents the state of the art in making velocity fluctuation measurements in the sea with adequate resolution so that the fluctuating components of the velocity can be separated from the mean flow. In the second part of this study, the results of field work in a near shore boundary layer using the instrument are presented. The analysis of the data set from this field study demonstrates the unique capabilities of this tool for making inroads into the study of marine boundary layers. Clearly, advances in our understanding of geophysical boundary layers depend on the ability to make measurements of the type described in this last section.

1.1 Turbulent Boundary Layer Scales

One of the difficulties in investigating turbulent boundary layers is the presence of a multiplicity of length scales. It is the purpose of this section to summarize the various scaling parameters in a steady, horizontally homogeneous, unstratified, turbulent boundary layer. In the ocean all of the above assumptions are generally violated as a whole or individually. However, the simple model developed from such a discussion provides a useful foundation to help understand what characteristics a velocity sensor must have in order to make successful measurements in marine boundary layers. It also helps in understanding the limitations involved in making boundary layer measurements.

Most of the large scale boundary layer flows in nature such as in estuaries, in the atmosphere, and near the ocean bottom are turbulent and time dependent. The characteristically high Reynolds numbers associated with such flows are a consequence of their large length scales. The early work on high Reynolds number boundary layers was performed in fluid mechanics laboratories. The discussion to follow is based on these laboratory studies. A detailed treatment of turbulent boundary layers can be found in standard texts such as Schlichting (1968) or Tennekes and Lumley (1972), or in classical works such as Clauser (1956).

One way of treating the problem of multiple length scales is to consider the scaling parameters of the flow starting at the solid boundary and continuing upwards to the free surface.

At the solid boundary, an assumption must be made about the geometry of the wall. Assuming for the moment a flat, mirror-smooth surface, the no slip boundary condition requires the existence of a region near the solid wall where viscosity must play a role. Physically, the flow is retarded near the wall and this fluid-solid interaction manifests itself as a shear stress on the boundary. This bottom shear stress, τ_b, may be used to define the friction velocity, u_*, defined as,

$$u_* \equiv \left(\frac{\tau_b}{\rho}\right)^{1/2} \qquad (1.1)$$

where ρ is the fluid density. The friction velocity is not a directly observable quantity, but rather a characteristic scaling parameter in turbulent flows with the units of velocity.

An estimate of the length scale over which viscous effects are important is obtained from the ratio of the kinematic viscosity, $\nu(cm^2/sec)$, to the friction velocity, $u_*(cm/sec)$, that is,

$$\frac{\nu}{u_*} = L_\nu \qquad (1.2)$$

The shear stress in the fluid is of a viscous nature over a distance L_ν from the boundary, and so the bottom stress can be written:

$$\tau_b = \rho\nu \left.\frac{dU}{dz}\right|_{z=0} \qquad (1.3)$$

where U is the horizontal velocity and z is the vertical distance

coordinate up from the bottom. Substituting the definition of u_* given by Eq. (1.1) and integrating the above expression, a linear velocity distribution results:

$$\frac{U}{u_*} = \frac{u_* z}{\nu} \qquad (1.4)$$

Experimentally, it has been found that this relationship holds over a region which has a thickness on the order of $5\nu/u_*$ (Schlichting, 1968). This region in which viscosity dominates is called the viscous sublayer.

Relaxing the assumption of a smooth boundary, and introducing roughness elements of a characteristic length, k_b, on the solid wall can cause dramatic changes in the flow near the wall. When $k_b < 5\nu/u_*$, the flow is termed hydrodynamically smooth. If the scale of the roughness elements approaches the characteristic dimension of the viscous sublayer; that is, if $k_b > 5\nu/u_*$, then the sublayer cannot form because it is broken up by the turbulence shed from the roughness elements. The flow is said to be in a transitional regime between hydrodynamically smooth and rough flow when $5 < u_* k_b/\nu < 70$. Completely rough turbulent flow exists when $u_* k_b/\nu > 70$; $u_* k_b/\nu$ is often called the roughness Reynolds number (Nikuradse, 1933) and is seen to be the ratio of sublayer thickness to the roughness height.

For practical situations in the ocean, ν/u_* is usually much smaller than the bottom roughness scale, and so a viscous sublayer would not be expected; however even in the case of $\nu/u_* > k_b$,

the sublayer thickness would be on the order of millimeters which would indeed be a challenge to the observationalist.

In the case of a rough boundary for which $\nu/u_* \gg k_b$, the length scale in the wall region is k_b. As the distance from the wall is increased, the effects of the boundary become less pronounced, and eventually the flow is unaffected by the wall's presence. Ultimately rotational or stratification effects become dominant and determines the thickness of the layer. At this distance the scaling length is the thickness of the boundary layer itself. Typically this boundary layer thickness, δ, is arbitrarily defined as the point where the mean horizontal velocity is 98% of the free stream velocity.

Three scaling lengths have now been identified, ν/u_*, k_b, and δ. The boundary layer thickness is many times larger than the roughness length or sublayer thickness, and since the range of separation of the two scales is so great, there is a region away from the boundary where k_b is too small to be dynamically important and δ is too large to have any effect. This level where the vertical separation from the boundary, z, satisfies both $z/k_b \gg 1$ and $z/\delta \ll 1$ is called the inertial sublayer. The scaling parameter for length in the inertial sublayer is simply z, the distance from the boundary. This region is characterized by the absence of significant viscous effects, and the shear stresses are due to the turbulent velocity fluctuations. These turbulent stresses will be discussed in detail later in this chapter, but at present it should be mentioned that these stresses scale as u_*^2, and that they are approximately

constant in the inertial sublayer as can be shown from the equations of motion (see for example the discussion in Tennekes and Lumley (1972) pp. 149-153). Many experiments carried out in flumes, wind tunnels, and pipes have shown that in the inertial sublayer the velocity distribution is logarithmic. These types of observations formed the impetus for the work of von Karman and Prandtl. Theodore von Karman in 1930 first derived the logarithmic profile for hydrodynamically smooth flow using a similarity argument. Prandtl subsequently developed the logarithmic velocity distribution for hydrodynamically rough conditions using a mixing length approach.

Assuming a layer of constant stress, the variation of mean velocity with height can be expressed in terms of the scaling parameters of the inertial sublayer; u_* is the relevant velocity scale and z the length scale:

$$\frac{dU}{dz} = \frac{c u_*}{z}$$

where c is a constant. This expression integrates to

$$\frac{U}{u_*} = c_0 \ln z + c_1 \qquad (1.5)$$

where c_0 and c_1 must be determined experimentally. The constant, c_0, is usually written $\frac{1}{\kappa}$, κ being von Karman's constant which is approximately equal to 0.4 for clear water. Suspended material in the flow tends to decrease the value of κ, and values as small as .26 have been reported (Raudkivi, 1967).

The empirically determined constant, c, is related to the roughness of the boundary, and the logarithmic velocity profile is usually written in a form that reflects this

$$\frac{U}{u_*} = \frac{1}{\kappa} \ln \frac{z}{z_o} \qquad (1.6)$$

where z_0 is a parameter reflecting the roughness height for the boundary. Over a rough boundary z_0 has been shown by experiments to be dependent on the characteristic dimension of the roughness elements, k_b, by the relation

$$z_o = \frac{k_b}{N}$$

where N depends on the roughness Reynolds number of the flow and k_b is the equivalent sand grain roughness (Nikuradse, 1933). For completely rough turbulent flow N is equal to 30; while for transitional flows it has a value near 22.

The above model of the logarithmic boundary layer profile has been derived for steady unstratified flow which is free of suspended matter and is horizontally homogeneous. If these assumptions are violated, deviations from logarithmic behavior would be expected. Stratification could put a lid on the log layer and shorten its vertical extent; while suspended material would decrease κ and thus alter the slope of the log profile.

Two other length scales in the boundary layer should be mentioned since they would be important depending on the situation

under analysis. The smallest scale of eddies which should exist represents the scale at which the eddies are dissipated by viscosity. In the inertial sublayer this length scale, known as the Kolmogorov fine scale, is given by

$$L_K = \left[\left(\frac{\nu}{u_*}\right)^3 \kappa z\right]^{1/4} \qquad (1.7)$$

where z is the vertical distance from the boundary (Tennekes and Lumley, 1972).

On a much larger scale, oceanic and atmospheric flows feel the effects of the earth's rotation. The scaling velocity can still be taken as u_* but the length scale must take the Coriolis parameter, $f(sec^{-1})$, into account. The thickness of this layer, called the Ekman layer, would then be on the order of u_*/f. Wimbush and Munk (1971) estimate the Ekman layer height to be $\kappa u_*/f$. If the Coriolis force is indeed felt, as in the case of an ocean basin with great horizontal extent, then theory shows (for example Tennekes and Lumley, 1972) that the velocity vector will deflect towards the right with increasing distance from the bottom in response to the Coriolis force. Monin and Obukhov (1954) indicate the height of the constant stress layer as

$$\delta_{\tau=\text{constant}} = \frac{.2\,u_*^2}{U_\infty f}$$

where U_∞ is the free stream velocity.

In tidal flows and for boundary layers under waves, the radian wave frequency, ω, scales the boundary layer thickness as,

$$\delta \sim \frac{\kappa u_*}{\omega}$$

where κ is von Karman's constant and $\omega = 2\pi/T$, T being the period of the oscillation. These flows have been investigated by Kajiura (1964), Grant and Madsen (1977), and Smith (1977).

Table 1.1 (in part from Wimbush, 1976) and Figure 1.1 illustrate order of magnitude estimates of the various layer thicknesses in three flow regimes in the ocean.

Note the critical dependence on u_* in the calculations leading to Table 1.1. The next section (1.2) will describe the methods used to obtain u_*. The above discussion on the structure of the boundary layer is based largely on measurements executed under laboratory conditions in which the mean flow was fully developed, stationary, neutrally stable and horizontally homogeneous.

In the ocean the mean flow is constantly changing and, depending on location, the fluctuations can be over time scales ranging from seconds to months. The in situ measurements of Heathershaw (1974) and Gordon (1974) have demonstrated that turbulent fluctuations occur intermittently near the boundary and hence the transport processes in the boundary layer require careful time series analysis. This concept of intermittency must be kept in mind when dealing with the dynamics of the boundary. Intermittency as it relates to the present study will be treated in a later section (1.2.4).

TABLE 1.1: Boundary Layer Scales (in part from Wimbush, 1976)

Regime	Quiescent Ocean Basin	Rise, Slope, Shelf	Intense Currents
Mean velocity U_∞	10^{-2} m/sec	10^{-1} m/sec	1 m/sec
Friction velocity $u_* \sim \frac{U_\infty}{10}$	10^{-3} m/sec	10^{-2} m/sec	10^{-1} m/sec
Thickness of sublayer $\delta_\nu \sim 5\frac{\nu}{u_*}$	8×10^{-3} m	8×10^{-4} m	8×10^{-5} m
Thickness of constant stress layer $\delta_{\tau=c}$	2×10^{-1} m	2 m	20 m
Reynolds stress $\tau(z) \sim \rho u_*^2$	10^{-3} dyn/cm^2	10^{-1} dyn/cm^2	10 dyn/cm^2
Thickness of logarithmic layer $\delta_L \sim \frac{.1u_*}{f}$	1 m	10 m	100 m
Thickness of Ekman layer δ_E	4 m	40 m	400 m
Kolmogorov fine scale at $\delta_{\tau=c}$	4×10^{-3} m	1.5×10^{-3} m	4×10^{-4} m

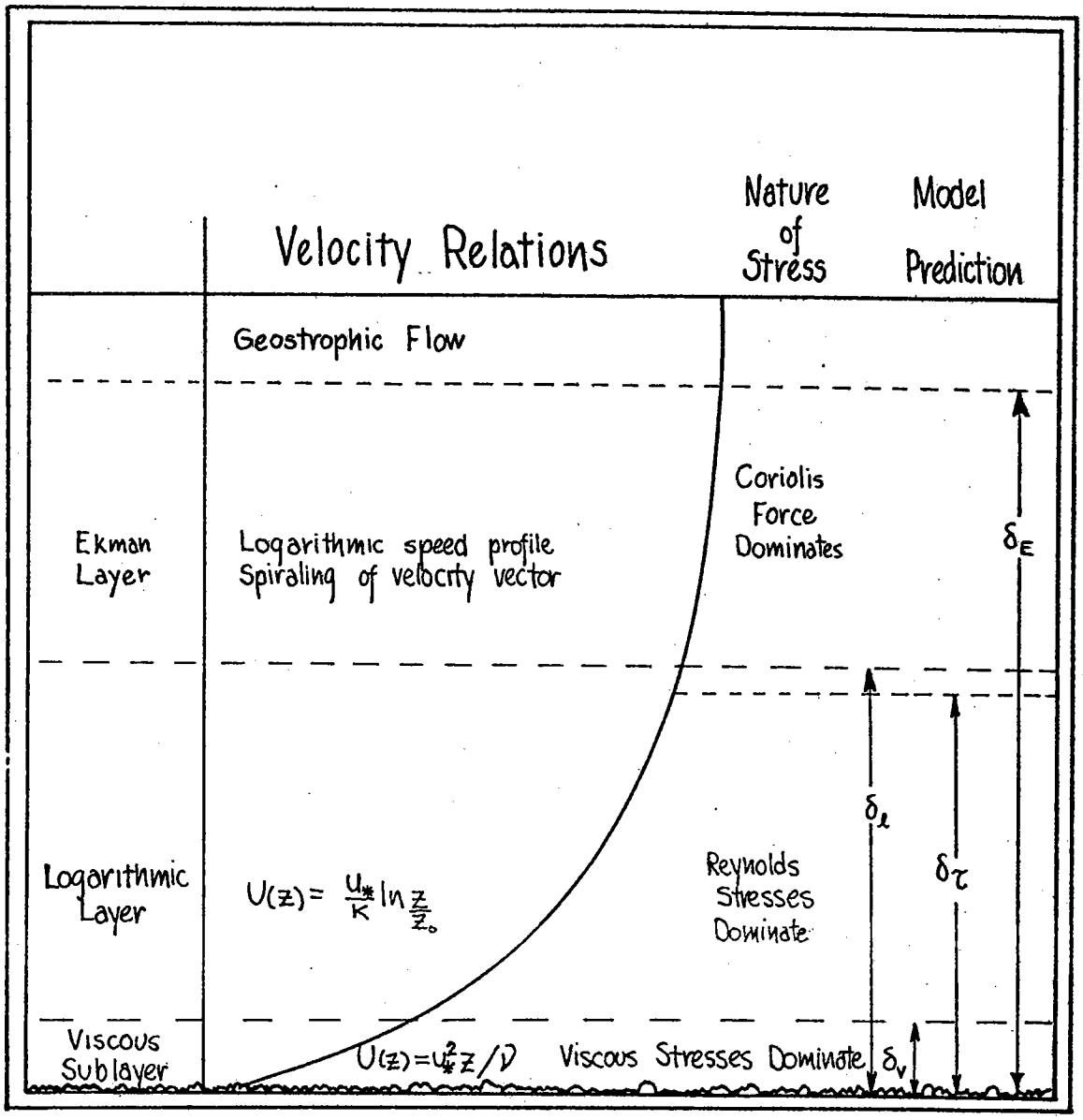
Velocity Relations
Nature of Stress
Model Prediction
Geostrophic Flow
Ekman Layer
Logarithmic speed profile
Spiraling of velocity vector
Coriolis Force Dominates
δ_E
δ_ℓ
δ_τ
Logarithmic Layer
$U(z) = \frac{u_*}{\kappa} \ln \frac{z}{z_0}$
Reynolds Stresses Dominate
Viscous Sublayer
$U(z) = u_*^2 z / \nu$
Viscous Stresses Dominate
δ_v

Figure 1.1

The field research undertaken to demonstrate capabilities of the instrumentation system developed for this thesis was performed in a shallow water ($\sim$ 10 m) tidal current. The question raised is: What can the type of data from this instrument say about how well current boundary layer models describe unsteady flow in shallow water? It is expected that the value of u_* will be a time varying function which should reflect the state of the tide (Kajiura, 1964). Since the bottom stress is proportional to the friction velocity, this has important implications for sediment transport in tidal currents.

In contrast to the deep ocean, the flow in a shallow tidal channel will exhibit no veering of the velocity vector since the sides of the channel will prohibit the effect of the Coriolis force from being significant to the dynamics of the flow. The driving force in shallow water in the case investigated is the pressure gradient due to the tide since no wind was present; and under quasi-steady conditions, a linear shear stress distribution will result ranging from zero at the free surface in the absence of wind to a maximum at the sediment-water interface.

Although the hydraulic forcing for the shallow water channel is different from that of the deep ocean, a constant stress layer near the bottom is expected which in turn would result in a logarithmic velocity profile when the flow is fully developed. In the absence of stratification, the logarithmic profile might be expected to exist throughout the water column except close to the free surface; however, it is more probable that in an actual experiment, the density structure

or the topography will dictate the height of the logarithmic layer.

It is anticipated that the flow will be intermittent and that analyses of the velocity fluctuations will reveal events responsible for large amounts of momentum transport, and that these events will have a multiplicity of scales.

Keeping the foregoing model and these expected results in mind, a discussion of previous experiments and methods of analysis is in order.

1.2 Background to Methods of Investigation and Previous Work

In this section, the methods which have been used to investigate the structure of the boundary layer in the marine environment are discussed. The target of these investigations predominately has been an appropriate value for the bottom shear stress, τ_b. Inherent in the analyses are important results with regard to length and time scales in the boundary layer.

1.2.1 Quadratic Drag Law

Classically, the determination of the shear stress at the bottom boundary in channel flow is made by measuring the mean horizontal velocity over the bottom and then invoking a quadratic drag law of the form:

$$\tau_b = C_f \rho \frac{U^2}{2} \qquad (1.8)$$

where τ_b = bottom shear stress

c_f = drag coefficient

ρ = fluid density

U = mean horizontal velocity

Implicit in this approach are the assumptions of steady flow and no density stratification. The empirical constant, c_f, can be determined with the flow similitude approach of using historical flume data obtained at the same roughness Reynolds number. As an example, in Vineyard Sound there is a tidal current of $\sim$ 30 cm/sec at a level 100 cm above the gravel bottom (.5 - 1.0 cm dia. pebbles). Following the approach mentioned above and using data from the text-book of Daily and Harleman (1966), one obtains a frictional coefficient of 5.0×10^{-3} for the site in Vineyard Sound. Interestingly in 1959 Bowden, Fairbairn and Hughes (1958) made near bottom velocity measure-ments in a tidal current (U $\sim$ 30 cm/sec) off Red Wharf Bay in North Wales. At that location the bed was composed of firm sand and shingle. By using the logarithmic profile technique (to be discussed in the next section), they obtained a value of $c_f = 7.0 \times 10^{-3}$ as defined by Eq. 1.8 for conditions similar to those described for Vineyard Sound. Their reference velocity was 1 meter.

Although the quadratic drag law oversimplifies the dynamics of the flow, it does lend itself to situations where horizontal velocity data is available from only one sensor near the bottom. It must be remembered that the drag coefficient is a function of Reynolds number and roughness, and that although it is constant when the boundary

layer is fully developed, it can vary considerably during periods when the flow is non-steady (Kajiura, 1964). Once a proper parameterization of the flow is made, future measurements can be simpler because the effects of roughness and turbulence can be treated through the drag coefficient.

1.2.2 Logarithmic Profile Method

> "The logarithmic velocity profile in the inertial sublayer is one of the major landmarks in turbulence theory. With analytical tools of a rather general nature a very specific result has been obtained, even though the equations of motion cannot be solved in general."
>
> (Tennekes and Lumley, 1972)

In section 1.1 the logarithmic profile in the inertial sublayer was derived, and can be written as

$$U(z) = \frac{u_*}{\kappa} \ln \frac{z}{z_0}$$

A plot of U versus the Naperian logarithm of z should yield straight lines whose slopes will give u_*/κ, and whose intercept with the U axis will yield z_0. A value of u_* can thus be found if a value for κ is assumed. It is taken to be 0.4 which is the clear water value.

Sverdrup (et al., 1942) has pointed out that measurements of velocity at two levels are necessary to obtain values of z_0 and u_* and measurements at three or more levels are required to validate the equation in the oceans. The first attempt at this was performed by Revelle and Fleming using a pendulum current meter at the entrance

of San Diego Harbor in 1937 (Sverdrup, et al., 1942). Measurements in the lower two meters in a tidal current of about 25 cm/sec showed good agreement with the log profile; frictional stress of 6 dynes/cm^2 were computed along with a bottom roughness of 2 cm.

Another pioneering study, this one more detailed, was made by Mosby in 1946, and again in 1949 (Mosby, 1946; Mosby 1949). Figure 1.2 is reproduced from his first paper. It shows mean velocity profiles during a five hour experiment in a strong tidal current north of Bergen, Norway. He found that for half hour averages of velocity the profile deviated from logarithmic but longer averages on the order of hours "may very well be interpreted by the usual logarithmic law" (Mosby, 1946). In Mosby's work is seen the surfacing of the time averaging problem which is to plague hydrodynamists, meteorologists and oceanographers in the decades to come.

Lesser (1951) also measured near bottom (< 2 m) mean velocities over differing bottom types and also found a good agreement to the log profile after suitable averaging similar to Mosby. More recently Wimbush and Munk (1970) report a logarithmic profile to a height of two meters above the bottom of the Pacific ($U \sim 5$ cm/sec). Sternberg (1970) on the other hand found that in the San Clemente Basin "many of the velocity profiles were not logarithmic thus precluding the analysis procedure." Quantitatively he estimates logarithmic profiles occurred between 22 and 57 percent of the time for his experiments off the California coast. Two possible causes for this could be unsteadiness in the boundary layer driving force, or multiple

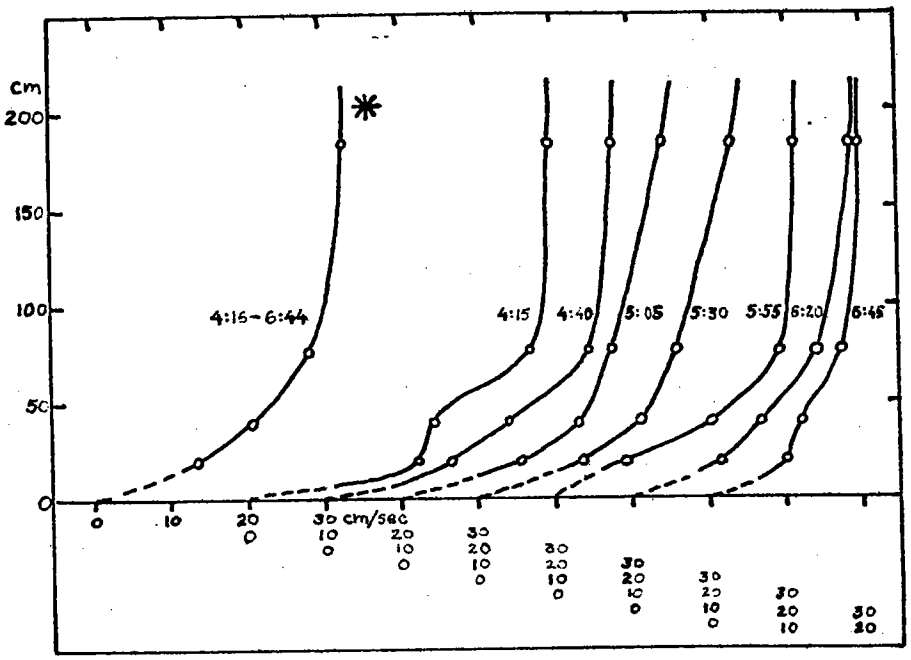

Mean Velocity Profiles (after Mosby, 1946)
25 minute averages
* is a 2½ hour average

Figure 1.2

roughness length scales as suggested by the work of Smith and McLean (1977). Their work shows that for a bed geometry exhibiting multiple roughness scales a series of logarithmic layers is expected. These layers are stacked vertically with each successive layer corresponding to an increasingly large length scale feature on the boundary. With these multiple scales, a simple mixing length argument based on only one length scale for the flow breaks down. Thus, it is not surprising that observation of a continuous logarithmic profile is elusive in regions where differing bottom length scales exist.

In contrast to this, various field investigations and a multitude of laboratory studies indicate that the logarithmic velocity distribution is a permanent feature in steady turbulent boundary layers, as in a laboratory flume or the atmosphere. The effects of the unsteadiness of the flow, the density structure, and the bottom topography must all be considered when attempting to fit oceanic observations to a steady, equilibrium boundary layer model.

1.2.3 Reynolds Stresses and Eddy Correlations

In this thesis a lower case letter with a tilde denotes the instantaneous value of a quantity; an upper case letter denotes a time averaged mean quantity; and a lower case letter represents the fluctuating component. Using this notation, the Reynolds decomposition of the time varying quantity, $\tilde{u}$, is defined as,

$$\tilde{u} = U + u$$

Figure 1.3 illustrates the coordinate system used throughout this thesis.

Proceeding from the equations of motion for an incompressible, viscous fluid, and using the continuity equation, one obtains the Navier-Stokes equations which then can be subjected to a Reynold's decomposition to give the steady state Reynolds momentum equation in tensor notation:

$$\rho U_j \frac{\partial U_i}{\partial x_j} = \frac{\partial}{\partial x_j}\left[-P\delta_{ij} + \frac{\mu}{2}\frac{\partial U}{\partial x_j} - \rho\overline{u_i u_j}\right] + F_i \qquad (1.9)$$

Mean Convection = pressure gradient + viscous stress + Reynolds stress + Body Forces

The overbar signifies a time average and

U_i, U_j = mean velocity components

u_i, u_j = fluctuating velocity components

ρ = density of the fluid

μ = molecular viscosity

P = time averaged pressure

i, j = coordinate indices 1 = x, 2 = y, 3 = z

F_i = body forces ($F_1 = F_2 = 0$, $F_3 = -\rho g$)

The vertical flux of momentum acts as an effective resistance to motion and an effective shear stress. Turbulent fluxes of momentum are known as Reynolds stresses.

Symbolically, the Reynolds stress tensor can be written as

$$\tau_{ij} = -\rho\overline{u_i u_j}$$

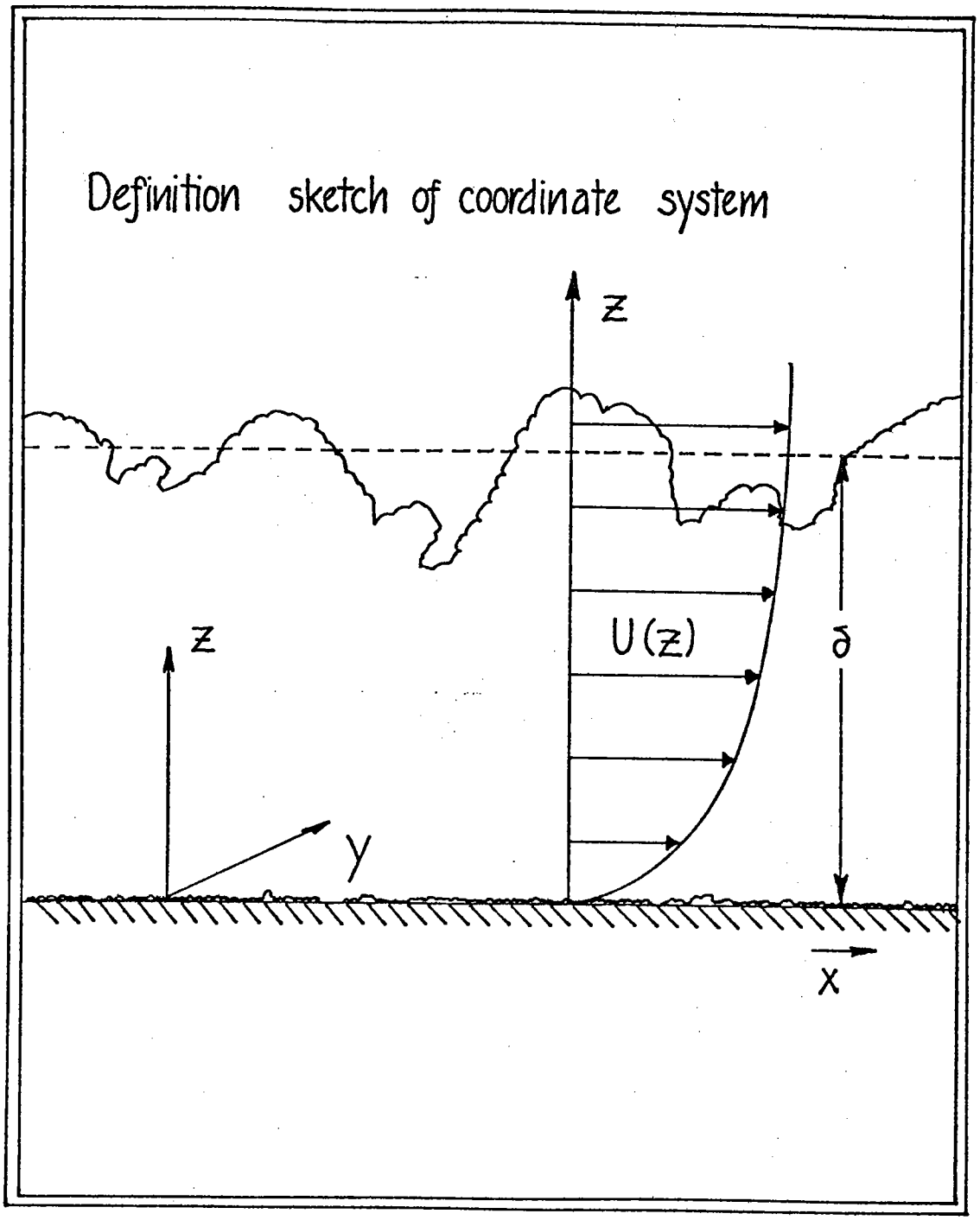

Figure 1.3